



## RESEARCH ARTICLE

# SYNTHESIS, MORPHOLOGICAL, OPTICAL CHARACTERIZATION OF PURE AND Co-DOPED TiO<sub>2</sub> NANOPARTICLES AND ITS ASSESSMENT TO ANTIMICROBIAL ACTIVITY

K. Manikandan<sup>a\*</sup>, A. Jafar Ahamed<sup>b</sup>, A. Thirugnanasundar<sup>c</sup>

<sup>a</sup>Department of Chemistry, Velalar College of Engineering & Technology, (Autonomous), Erode-638 012, India

<sup>b</sup>PG & Research Department of Chemistry, Jamal Mohamed College (Autonomous), Trichy-620 020, India

<sup>c</sup>Department of Chemistry, Erode Arts & Science College (Autonomous), Erode-638009, India

Received 3 March, 2017; Accepted 10 April 2017

Available online 19 April 2017

## Abstract

The pure and different weight % of cobalt doped TiO<sub>2</sub> nanoparticles were synthesized by sol-gel method and calcinated at 600°C for 5 h. The synthesized products were characterized by XRD, FESEM, EDXS and UV-Vis. and Photoluminescence study. XRD pattern of pure TiO<sub>2</sub>, 1 wt%, 3 wt% Co-doped TiO<sub>2</sub> nanoparticles confirms the anatase structure. The crystallite size of pure TiO<sub>2</sub> is 37 nm and 1 wt %, 3wt % Co-doped TiO<sub>2</sub> are 38 and 42 nm. The FESEM Micrograph shows the agglomerated particles of spherical-like morphology. Direct allowed band gap of pure and Co-doped TiO<sub>2</sub> nanoparticles studied by UV-Vis spectrometer. The photoluminescence spectra of pure and Co-doped TiO<sub>2</sub> shows the recombination of charge carriers is effectively reduced by the doping Cobalt metal. The Kirby Bauer Agar Well Diffusion Assay method was employed to explore antimicrobial activity of nanosized pure and Co-doped TiO<sub>2</sub> colloidal suspension against the test microorganism of gram positive bacteria (*B. subtilis*), gram negative Bacteria (*S. aeruginosa*) and one fungus (*A. niger*). The Co-doped TiO<sub>2</sub> nanoparticles inhibited shows that the multiplication and growth of the above mentioned test bacteria and fungi. Antimicrobial activity was found against all tested microorganisms and confirmed that Co-doped TiO<sub>2</sub> nanoparticles possess high antimicrobial activity at a concentration of range of 25, 50, 75 and 100 µg of 1wt%, 3wt% Co-doped TiO<sub>2</sub> solutions.

## Keywords

XRD

FESEM

UV-Vis.

Photoluminescence

Antimicrobial activity

\*Corresponding author Tel. +91 4242244201

FAX: +914242244205.

E-mail : chemmani03@gmail.com

## Introduction

TiO<sub>2</sub> is considered as a good semiconducting material compared to other semiconducting materials. Because, it possesses non-toxicity, chemical stability and high refractive index. Titanium dioxide exists in three different crystalline phases: rutile, anatase, and brookite. Rutile phase is a stable one compared to other two phases and others are in metastable. Rutile and anatase systems have tetragonal unit cells. The rutile phase has two TiO<sub>2</sub> molecules per unit cell having lattice constant  $a=4.59 \text{ \AA}$  and  $c=2.95 \text{ \AA}$  and the anatase phase has four TiO<sub>2</sub> molecules per unit cell having lattice constant  $a=3.78 \text{ \AA}$  and  $c=9.51 \text{ \AA}$ . Generally, TiO<sub>2</sub> nano crystal has been changed from anatase to rutile structure when the increase temperature to above 450°C [1,2]. Band gap value of the anatase phase is higher than that of the rutile phase, so the properties of rutile are slightly better than the anatase phase properties in semiconducting performance [3].

Generally, TiO<sub>2</sub> has been used in various fields of science and technology, especially in the pharmaceutical field and growingly attracted the attention of many researchers. Now, the scientists are focussed in TiO<sub>2</sub> nanoparticles on antimicrobial activity is due to its rapid recombination of photo activated electrons and positive holes. In the last decade, researchers give more attention on the antimicrobial activity of doping of titanium dioxide with transition metals like tungsten, cobalt etc. There are different methods like sol-gel synthesis [4], ion-impregnation [5], and hydrothermal synthesis [6] to get homogeneous doping of cobalt in TiO<sub>2</sub>. Sol-gel is the very simple and sophisticated method proposed by Byun *et al.* [7] among the various methods for producing nanoparticles. In this present study, Co-doped TiO<sub>2</sub> nano ranged particles prepared by sol-gel method is to study the effect of cobalt doping on the morphology, crystal structure, optical properties and find the highest possible antimicrobial activity of pure and cobalt doped TiO<sub>2</sub> nanoparticles. In this work, pure and Co-doped TiO<sub>2</sub> were characterised by different techniques X-ray diffraction (XRD), Field Emission Scanning Electron Microscopy (FE-SEM), Energy Dispersive X-ray spectroscopy (EDXS), UV-Visible Diffuse Reflectance Spectroscopy (UV), Photoluminescence analysis (PL). The Kirby Bauer Agar Well Diffusion Assay method was employed to analyse antimicrobial activity of nanosized pure and Co-doped TiO<sub>2</sub> nanoparticles against the test microorganisms gram positive bacteria (*B. subtilis*), gram negative bacteria (*P. aeruginosa*) and fungi (*A. niger*). Antimicrobial activity was found against all above mentioned microorganisms by pure and Co-doped TiO<sub>2</sub> nanoparticles.

## Experimental

### Materials

Titanium isopropoxide (Sigma-Aldrich), cobaltous sulphate heptahydrate (Merck), Ethanol (German), hydroxylamine hydrochloride (Sigma-Aldrich) were used as precursor without any further purification. Doubly distilled water was used for the whole synthesis process. Bacterial cultures such as *B. subtilis*, *P. aeruginosa* and fungus culture as *A. niger* were obtained from Eumic Analytical Lab and Research Institute, Tiruchirappalli. Bacterial strains were maintained on nutrient agar slants (Himedia) at 4°C.

### Physicochemical characterization

The XRD pattern analysis for pure TiO<sub>2</sub> and doped TiO<sub>2</sub> nanoparticles was recorded by Lab X XRD6000 Shimadzu model with Cu-K $\alpha$  radiation. The structure and morphology of the nanoparticles were investigated by FE-SEM using FEI Quanta FEG 200-High Resolution Scanning Electron Microscope. The absorption spectra and optical band gap of the TiO<sub>2</sub> and doped TiO<sub>2</sub> nanoparticles samples were measured by using UV-Vis. spectrophotometer (JASCO U-670 Spectrometer) and alcohol as a solvent. The spectrum was recorded between 200 - 800 nm. A PL spectrum was recorded between 370-770 nm and it was carried out by using Horiba Jobnyvon model spectrophotometer and the alcohol was used a solvent. EDXS analysis was carried out to find out the composition of JE2100 (JEOL-200KV, LB6 filament) pure and doped TiO<sub>2</sub> samples by using the detector attached with the same instrument.

### Preparation of pure TiO<sub>2</sub> and Co-doped TiO<sub>2</sub> nanoparticles

Pure titanium dioxide nanoparticles of wt 1%, 3% Co-doped TiO<sub>2</sub> nanoparticles were prepared by sol gel method. The preparation of TiO<sub>2</sub> nanoparticles can be carried out by using aqueous solution of titanium(IV) isopropoxide as starting material. The sol was prepared by mixing titanium isopropoxide (3ml) with 24 ml of Ethanol and dissolved 1000 ml of double distilled water at room temperature. The molar ratio of titanium isopropoxide and alcohol is 1:8 respectively. 1 g of hydroxylamine hydrochloride was dissolved in 100 ml of deionised water and added gradually to the titanium isopropoxide sol. After stirring, an aqueous solution was centrifuged by using centrifuge machine. The precipitate obtained was dried at 105°C in hot air oven. It was then calcinated at 600°C in a muffle furnace for 5 h at a constant temperature rise of 2°C/min.

The preparation of wt1%, 3% Co-doped TiO<sub>2</sub> nanoparticles can be carried out by using aqueous solution of titanium(IV) isopropoxide as starting material. The sol was prepared by mixing titanium isopropoxide (3 ml) with 24 ml of Ethanol and dissolved 1000ml of double distilled water at room temperature. The molar ratio of titanium isopropoxide and alcohol is 1:8 respectively. 1 g of hydroxylamine hydrochloride was dissolved in 100 ml of deionised water and added gradually to the titanium isopropoxide sol. To synthesis the cobalt doping, wt1% of solution was added into the TiO<sub>2</sub> sol. The mixture of titanium (IV) isopropoxide and cobaltous sulphate heptahydrate solutions were stirred for 3 h. After stirring, an aqueous solution was centrifuged by using centrifuge machine. The precipitate obtained was dried at 105°C in hot air oven. It was then calcinated at 600°C in a muffle furnace for 5 h at a constant temperature. Similarly, the same procedure was followed for the synthesis of wt3% Co-doped TiO<sub>2</sub> nanoparticles.

### **Antimicrobial activity**

#### *Preparation of culture media*

Nutrient agar medium of pH 7 is one of the most commonly used medium for several routine bacteriological purposes. It was prepared by dissolving 5 g of peptone, 3 g of beef extract, 15 g of Agar, 5 g of sodium chloride, 1.5 g of yeast extract in 100 ml of distilled water, it is boiled to dissolve the medium completely and sterilized by autoclaving at 15 Ib psi pressure (121°C) for 15 min.

#### *Inoculum preparation*

Bacterial cultures were subculture in liquid medium (nutrient broth) at 37°C for 8 h and further used for the test (10<sup>5</sup>-10<sup>6</sup> CFU/ml). The suspensions were prepared before the test was carried out.

#### *Assay of antimicrobial activity*

The nutrient broth was prepared, and bacterial and fungal colonies were inoculated into the broth culture and are used to assay the antimicrobial activity.

#### **Inhibition zone assay**

The nutrient agar medium was prepared and sterilized by autoclaving at 121°C 15 lbs pressure for 15 min., then aseptically poured the medium into the sterile

petriplates and allowed to solidify the bacterial and fungal broth culture was swabbed on each petriplates using a sterile buds. Then, wells were made by well cutter. wt1%, 3% Co-doped TiO<sub>2</sub> nanoparticles containing solutions were prepared dissolving 100 mg of each in 100 ml of DMSO solvent and from this stock solution, different concentrations of wt1%, 3%, Co-doped TiO<sub>2</sub> nanoparticles calcinated at 600°C (25, 50, 75 and 100 µg) solutions were taken for assay.

The antimicrobial activity of 1wt%, 3wt% Co-doped TiO<sub>2</sub> nanoparticles calcinated at 600 °C were assayed against *B. subtilis*, *P. aeruginosa* and *A. niger* at 37°C for 24 h. After incubation the plates were observed for the zone of inhibition.

The bacterial and fungal viable count was determined after 24 h by plating wt1%, 3% Co-doped TiO<sub>2</sub> nanoparticles calcinated at 600°C on nutrient agar plates and the number of colony forming units (CFU) which were counted by a viable count method. To control this, the bacterial and fungal cultures were incubated with gentamicin. The diameter zone of inhibition was measured and expressed in millimetre (mm)[8].

Kirby Bauer Agar Well Diffusion Assay test was conducted using wt1%, 3% Co-doped TiO<sub>2</sub> nanoparticles calcinated at 600°C nanoparticles and common antibiotic Gentamicin. The diameter zones of inhibition for wt1%, 3% Co-doped TiO<sub>2</sub> nanoparticles were compared to this antimicrobial agent [9]. The diameter of zone of inhibition for pure TiO<sub>2</sub> at 600°C was also compared to this antimicrobial agent. To analyse the antimicrobial activity of wt1%, 3% Co-doped TiO<sub>2</sub> nanoparticles calcinated at 600°C was obtained by the micro emulsion method.

## **Results and discussion**

### **X-ray diffraction**

XRD Analysis was used to find the crystalline phase and the structure of the synthesised nanoparticles. Fig. 1(a-c) shows the XRD pattern of pure and cobalt doped TiO<sub>2</sub> nanoparticles. The results shows that the pure TiO<sub>2</sub> nanoparticles calcinated at 600°C

confirms the formation of anatase phase by the existence of strong diffraction peaks at  $2\theta$  values of  $25.3^\circ$ ,  $38.44^\circ$ ,  $48^\circ$ ,  $54^\circ$ ,  $55.07^\circ$ ,  $63^\circ$ ,  $69.23^\circ$ ,  $70.89^\circ$  and  $75.38^\circ$  corresponding to the crystal planes of (101), (112), (200), (105), (211), (204), (116), (220), and (215) respectively.  $\text{TiO}_2$  nanoparticles calcinated at  $600^\circ\text{C}$ . This indicates the formation of anatase phase of titanium dioxide [JCPDS Card No 21-1272] belonging to the tetragonal structure. The XRD patterns obtained for 1 wt %, 3 wt % cobalt doped  $\text{TiO}_2$  nanoparticles were shown in the figure 1(b, c). Addition of 1wt %, 3 wt% of cobaltous sulphate hepta hydrate did not affect the crystal structure of the titania. All the peaks are present in the XRD pattern of co-doped  $\text{TiO}_2$  shows the characteristics diffraction peaks of anatase phase which is similar to XRD pattern of pure  $\text{TiO}_2$ . The results obtained for the wt1%, 3% cobalt doped  $\text{TiO}_2$  nanoparticles calcinated at  $600^\circ\text{C}$  confirms the formation of anatase phase by the presence of strong diffraction peaks at  $2\theta$  values of  $25.3^\circ$ ,  $38.44^\circ$ ,  $48^\circ$ ,  $54^\circ$ ,  $55.07^\circ$ ,  $63^\circ$ ,  $69.23^\circ$ ,  $70.89^\circ$  and  $75.38^\circ$  corresponding to the crystal planes of (101), (112), (200), (105), (211), (204), (116), (220), and (215), respectively. This indicates the formation of anatase phase of  $\text{TiO}_2$ .

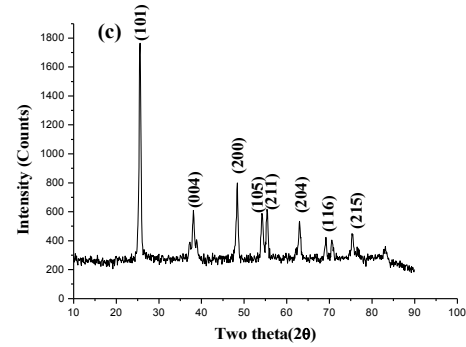
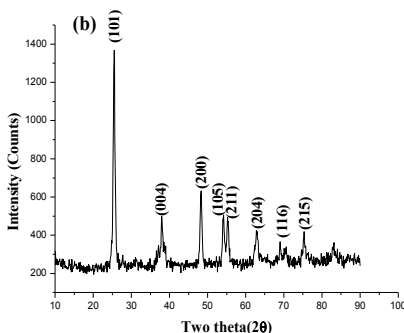
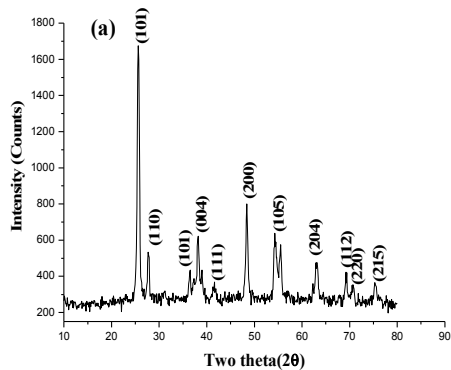


**Fig. 1.** XRD patterns of (a) pure  $\text{TiO}_2$  (b) 1 wt% Co-doped  $\text{TiO}_2$  (c) 3 wt % Co-doped.

This XRD pattern of the present study was reported in the earlier study (Karthik *et al.*, 2010) [10]. This wt1%, 3% doping cobalt incorporation do not show any cobalt phase in cobalt-doped  $\text{TiO}_2$  XRD pattern which indicates that cobalt ions are uniformly distributed on the host  $\text{TiO}_2$ . The average particle sizes of pure  $\text{TiO}_2$  powder is a  $\sim 37$  nm. The average particle size of 1 wt %, 3 wt % Co- $\text{TiO}_2$  powders are about 38 and 42 nm respectively. The average particle size was calculated using the following Debye-Scherrer's formula,

$$D = K \lambda / \beta \cos \theta$$

In this equation, D is the crystallite size, K the Scherrer constant usually taken as 0.89,  $\lambda$  the wavelength of the X-ray radiation (0.15418 nm for  $\text{Cu K}\alpha$ ).

### Field Emission Scanning Electron Microscopy

FE-SEM Fig. 2(a-c) images of pure and wt1%, 3% co-doped  $\text{TiO}_2$  nanoparticles calcinated at  $600^\circ\text{C}$ . From the figures, it can be confirmed that the average agglomerated particle size of pure  $\text{TiO}_2$  is 37 nm with nearly spherical and uniform sized particles.

FE-SEM images of the cobalt doped  $\text{TiO}_2$  nanoparticles shows most of the nanoparticles are almost uniform and spherical sized particles, coherent together and also closer view shows that spherical particles are clearly seen due to nano cluster formed during the growth. These spherical shaped particles are agglomerated particles in the range of 38 to 42 nm.

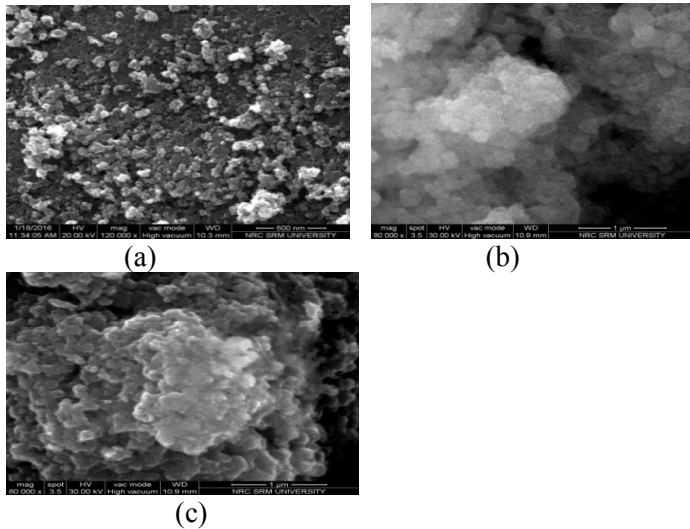


**Figure 2.** FE-SEM micrographs of (a) pure  $\text{TiO}_2$ , (b) 1 wt % Co-doped  $\text{TiO}_2$ , (c) 3 wt % Co-doped  $\text{TiO}_2$  nanoparticles calcinated at  $600^\circ\text{C}$ .

### Energy Dispersive X-ray Spectroscopy

Analysis of EDXS is used to analyse the chemical composition of the prepared material. It is clear that from Fig. 3(a)  $\text{TiO}_2$  is in pure form and free from any observable impurities. Fig. 3(b, c) also shows the EDXS of 1 wt %, 3 wt % Co-doped  $\text{TiO}_2$  samples, prepared by sol-gel method. EDXS shows only peaks of titanium, cobalt and oxygen elements. From the figure, it is clear that Co-doped  $\text{TiO}_2$  is free from impurities.

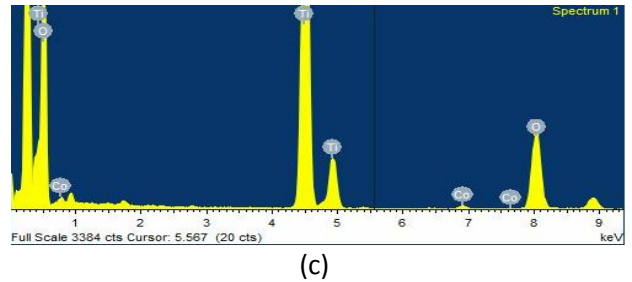
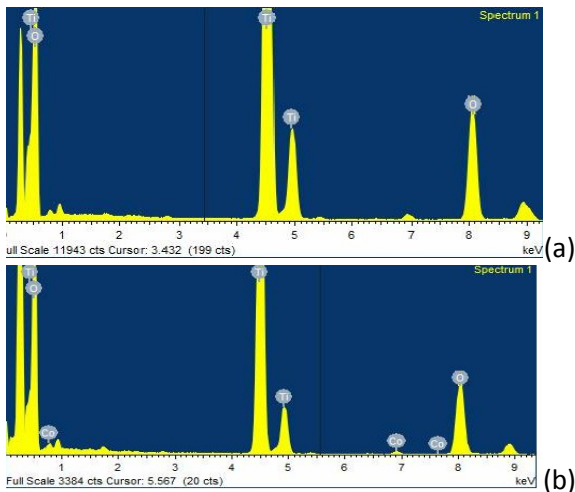


**Fig. 3.** EDXS pattern of (a) pure  $\text{TiO}_2$  (b) 1 wt % Co-doped  $\text{TiO}_2$  (c) 3 wt % Co-doped  $\text{TiO}_2$  nanoparticles calcinated at  $600^\circ\text{C}$ .

### UV-Visible diffuse reflectance spectra

UV-Visible spectroscopy helps to understand the optical properties and bandgap of nanoparticles. The UV-Visible spectra of pure  $\text{TiO}_2$ , 1 wt %, 3 wt % Co-doped  $\text{TiO}_2$  nanoparticles is shown in the Fig. 4. The absorbance can vary depending upon some factors like particle size, oxygen deficiency, defects in material prepared, *etc* [11]. It was recorded in the range of 200 to 800 nm.

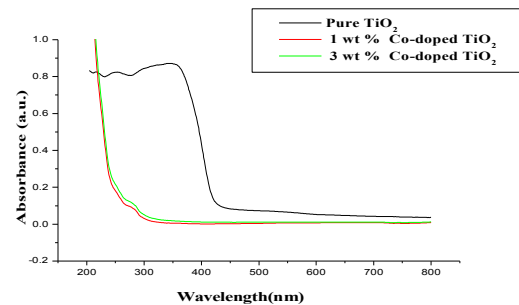


**Fig. 4.** UV-Vis diffuse reflectance spectra of pure and Co-doped  $\text{TiO}_2$  nanoparticles calcinated at  $600^\circ\text{C}$ .

The UV-Visible spectrum of pure  $\text{TiO}_2$  obtained at 350 nm attribute to charge-transfer from the valence band formed by 2p orbitals of the oxide anions to the conduction band formed by the 3d orbitals of the  $\text{Ti}^{4+}$  cations [12,13]. It was also observed from the figure 4 the absorption is shift towards the lower wavelength side for pure  $\text{TiO}_2$  compared with Co-doped  $\text{TiO}_2$  samples due to blue shift in absorbance. But in the case of UV-Vis. absorbance spectra of doped  $\text{TiO}_2$ , 1 wt % Co-doped  $\text{TiO}_2$  compared with other 3 wt % Co-doped  $\text{TiO}_2$  samples observed redshift. It can also be seen that from the Fig. 4 optical absorption edges were shifted to higher wavelength region (red shift) with increasing dopant cobalt. The absorption of Co-doped samples of  $\text{TiO}_2$

shifted to visible region attributed to the d-d electron in transition of  $\text{Co}^{2+}$  in octahedral coordination.

The band gap of the samples can be determined by extrapolation of the absorption edge onto the x-axis and using the Planck's equation  $E_g = hc/\lambda$ , where  $E_g$  is the energy gap of pure and doped  $\text{TiO}_2$  at absorption wavelength  $\lambda$ ,  $h$  is the Planck's constant,  $C$  is the velocity of light.

The calculated bandgap value of pure  $\text{TiO}_2$  is 2.86 eV and Co-doped nanoparticles values are 4.90 and 4.56 eV. From the bandgap values of Co-doped  $\text{TiO}_2$ , decreases when increase in the doping of cobalt content which shift to the longer wavelength. The two mechanism may be responsible for the narrowing the band gap. The first one is new d-states are introduced near the valence band edge which narrow the band gap of the  $\text{TiO}_2$  system and the second is substitution of dopant  $\text{Co}^{2+}$  to the  $\text{Ti}^{4+}$  site introduced defect states related by oxygen vacancy in the forbidden energy band gap zone of  $\text{TiO}_2$ .

### Photoluminescence study

Photoluminescence spectroscopy is useful for finding the efficiency of trapping of charge carrier, transfer and circumstances of electron-hole pairs in semiconductor particles. The Fig. 5 shows the excitation wavelength of the pure  $\text{TiO}_2$  and doped  $\text{TiO}_2$  is found between 300 and 325 nm.

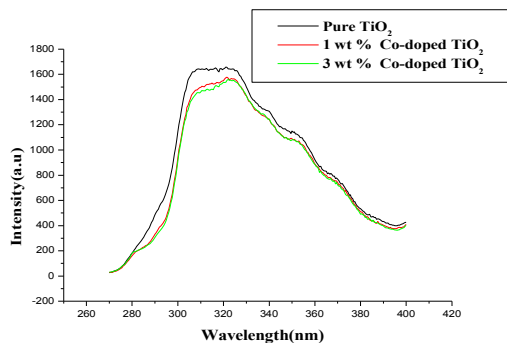


**Fig. 5.** Photoluminescence spectra of pure and Co-doped  $\text{TiO}_2$  nanoparticles calcinated at  $600^\circ\text{C}$ .

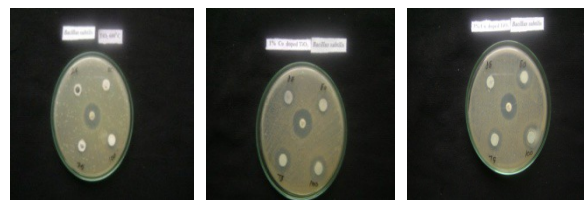
The excitation wavelength observed for pure  $\text{TiO}_2$  is 325 nm. Similarly, for other excitation wavelength of Co-doped  $\text{TiO}_2$  nanoparticles was observed at 325 nm which indicates that trapped electrons and oxygen vacancies. Fig. 5 also shows the photoluminescence intensity of pure  $\text{TiO}_2$  is greater of PL intensity than the 1 wt %, 3 wt % Co-doped  $\text{TiO}_2$ , which is due to a lower recombination rate of electrons and holes [14,15] in the presence of light

irradiation. It indicates that the recombination of charge carriers is effectively reduced by the doping cobalt metal [16].

### Antimicrobial activity

The antimicrobial activities of the samples were identified from the zone of inhibition. The results showed that for all of the four samples at different concentration showed some good zone of inhibition against all the pathogens used. In addition, it could be observed that the doped samples were having much higher zone of inhibition compared to the pure  $\text{TiO}_2$  sample. It shows that there was a significant effect of the cobalt induced antimicrobial activity for all the other doped samples. Also, the zone of inhibition increases as the concentration of the samples increases for almost all the samples against all the pathogens. However, none of the samples were able to reach the zone of inhibition of the standard gentamicin except for the one sample which showed some higher zone of inhibition against the gram positive bacteria. The 3 wt % Co-doped  $\text{TiO}_2$  at higher concentration (100 mg) showed a higher zone of inhibition against the gram positive bacteria *B. subtilis* compared to all other pure and doped samples including the standard Gentamicin. This result proved that the effect of the cobalt doping on  $\text{TiO}_2$  enhances the antimicrobial activity due to modified surface area, morphology and the reactivity of the samples.

#### (a) *Bacillus subtilis* (Gram positive)



Pure  $\text{TiO}_2$  calcinated at  $600^\circ\text{C}$

1 wt % Co-doped  $\text{TiO}_2$

3 wt % Co-doped  $\text{TiO}_2$

#### (b) *Pseudomonas aeruginosa* (Gram negative)



Pure  $\text{TiO}_2$  calcinated at  $600^\circ\text{C}$

1 wt % Co-doped  $\text{TiO}_2$

3 wt % Co-doped  $\text{TiO}_2$



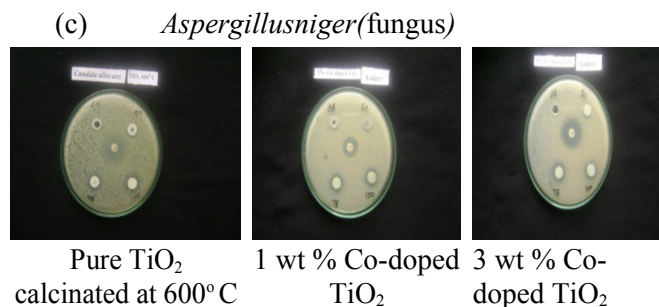


**Fig. 6.** Inhibition zone of different microorganism by media subjected to pure and Co-doped TiO<sub>2</sub> nanoparticles calcinated at 600°C.

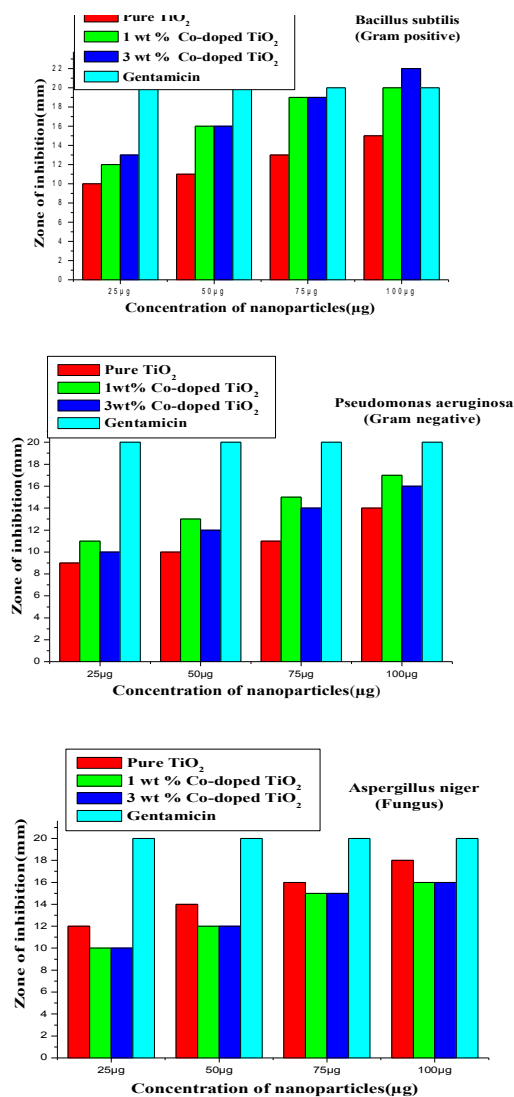


**Figure 7.** Antibacterial effect of pure and Co-doped TiO<sub>2</sub> nanoparticles calcinated at 600°C.

## Conclusions

Co-doped TiO<sub>2</sub> nanoranged particles successfully prepared by sol-gel method. XRD pattern of 1 wt %, 3 wt % cobalt doped TiO<sub>2</sub> did not show any cobalt phase which indicates that cobalt ions were uniformly distributed on the host TiO<sub>2</sub>. The average particle size of pure TiO<sub>2</sub>, wt 1%, and 3% Co-doped TiO<sub>2</sub> powders were about 37, 38, 42 nm respectively. FE-SEM image of Co-doped TiO<sub>2</sub> confirms that, spherical particles were clearly seen due to nano cluster formed during the growth. EDXS analysis shows, only Co, Ti and oxygen present, no impurities present in the Co-doped TiO<sub>2</sub> nanoparticles. UV-Vis., spectrum shows optical absorption edges were shifted to higher wavelength region (red shift) with increasing dopant cobalt. The absorption of Co-doped samples of TiO<sub>2</sub> shifted to visible region attributed to the d-d electron in transition of Co<sup>2+</sup> in octahedral coordination. Photoluminescence intensity of pure TiO<sub>2</sub> is greater than 1 wt %, 3 wt % Co-doped TiO<sub>2</sub>, is due to a lower recombination rate of electrons and holes the presence of light irradiation. It indicates that the recombination of charge carriers was effectively reduced by the doping cobalt metal. Cobalt doping on TiO<sub>2</sub> enhances the antimicrobial activity due to modified surface area, morphology and the reactivity of the samples.

## References

- [1] M.R. Hoffmann, S.T. Martin, W. Choi, W. Bahnemann, *Chem. Rev.*, 95, (1995), 69.
- [2] A. Fujishima, T.N. Rao, D.A. Truk, *J. Photochem. Photobiol. C Photochem. Rev.*, 1, (2000), 1.
- [3] S.D. Mo, W.Y. Ching, *Phys. Rev. B*, 51-19, (1995), 13023.
- [4] H. Yang, D. Zhang, L. Wang, *Mater. Lett.*, 57, (2002), 674.
- [5] Ramis, G. Busca, C. Cristiani, L. Lietti, P. Forzatti, F. Bregani, *Langmuir*, 8, (1992), 1744.
- [6] V. Stengl, J. Velicka, M. Marikova, T.M. Grygar, *ACS Appl. Mater. Interf.*, 3, (2011), 4014.
- [7] D. Byun, Y. Kim, K. Lee, P. Hofmann, *J. Hazard. Mater.*, 73(2), (2000), 199.
- [8] A.W. Bauer, M.M. Kirby, J.C. Sherris, M. Truck, *Am. J. Clin. Pathol.*, 45, (1966), 493.

- [9] A. Zielińska, E. Kowalska, J.W.Sobczak, I. Łacka, M. Gazda, B. Ohtani, *Sep. Purif. Tech.*, 72, (2010), 309.
- [10] K. Karthik, S.K. Pandian, K.S. Kumar, N.V. Jaya, *Appl. Surf. Sci.*, 256, (2010), 4757.
- [11] T.N. Soitah, Y. Chunhui, S. Liang, *Sci. Adv. Mater.*, 2, (2010), 534.
- [12] A. Ratnamala, G. Suresh, V.D. Kumari, V. Subrahmanyam, *Mat. Chem. Phys.*, 110, (2008), 176.
- [13] J.K. Reddy, G. Suresh, C.H. Hymavathi, V.D. Kumari, M. Subrahmanyam, *Catal. Today*, 141, (2009), 89.
- [14] S. Hu, F. Li, D.Z. Fan, *Bull. Korean Chem. Soc.* 33, (2012), 2309.
- [15] Y.L. Kuo, H.W. Chen, Y. Ku, *Thin Solid Films*, 515, (2007), 3461.
- [16] J. Liqiang, S.Xianojun, X.Baiqi, C.Weimin, F. Honggang, *J. Solid State Chem.*, 177, (2004), 3375.